

DNA-Intercalating Supramolecular Hydrogels for Tunable Thermal and Viscoelastic Properties

Shaina M. Hughes[†], Aylin Aykanat[†], Nicholas G. Pierini, Wynter A. Paiva, April A. Weeks, Austin S. Edwards, Owen C. Durant, and Nathan J. Oldenhuis^{*}

Abstract: Polymeric supramolecular hydrogels (PSHs) leverage the thermodynamic and kinetic properties of non-covalent interactions between polymer chains to govern their structural characteristics. As these materials are formed via endothermic or exothermic equilibria, their thermal response is challenging to control without drastically changing the nature of the chemistry used to join them. In this study, we introduce a novel class of PSHs utilizing the intercalation of double-stranded DNA (dsDNA) as the primary dynamic non-covalent interaction. The resulting dsDNA intercalating supramolecular hydrogels (DISHs) can be tuned to exhibit both endothermically or exothermically driven binding through strategic selection of intercalators. Bifunctional polyethylene glycol ($M_w \sim 2000$ Da) capped with intercalators of varying hydrophobicity, charge, and size (acridine, psoralen, thiazole orange, and phenanthridine) produced DISHs with comparable moduli (500–1000 Pa), but unique thermal viscoelastic responses. Notably, acridine-based cross-linkers displayed invariant and even increasing relaxation times with temperature, suggesting an endothermic binding mechanism. This methodology expands the set of structure-properties available to biomass-derived DNA biomaterials and promises a new material system where a broad set of thermal and viscoelastic responses can be obtained due to the sheer number and variety of intercalating molecules.

Polymeric supramolecular hydrogels (PSHs) are an important class of physical gels that exhibit useful properties such as tunable viscoelasticity, self-healing, and stimuli-responsiveness.^[1–4] These characteristics give PSHs diverse applications in drug delivery, tissue-mimicking materials, and 3D printing.^[5–7] The physical properties of PSHs, such as plateau modulus (G^0), gelation point (t_g), and relaxation

time (τ), are dictated by the equilibrium constant (K_{eq}), association rate (k_a), and dissociation rate (k_d) of the non-covalent interactions between polymers (Figure 1a).^[8–11] Thus, the cross-linking equilibrium must be highly favored, i.e. $\Delta G^\circ \ll 0$, to form a robust material. To achieve this, PSHs are often made exothermic ($\Delta H^\circ < 0$, $\Delta H^\circ \ll -T\Delta S^\circ$) by facilitating hydrogen bonding, metal-ligand interactions, or other energetically favorable interactions between polymers.^[12–19] Unfortunately, at high temperatures, the acceleration of unbinding shifts the equilibrium towards the reactants, causing PSHs to become viscous, thus limiting their applications. In contrast, Yu and co-workers demonstrated an endothermically driven ($\Delta S^\circ > 0$, $\Delta H^\circ > 0$) polymer-nanoparticle hydrogel that exhibited temperature-invariant viscoelasticity.^[21] Materials of this type rely on entropic forces, such as high configurational entropy or increases in translational entropy of solvents to drive gelation.^[21–24] While both enthalpically and entropically-driven supramolecular hydrogel formation are preceded, they require dramatically different compositions and physical interactions. This complicates the application of these materials, as achieving a desired set of mechanical properties could be negated by poor thermal response. Thus, demonstrating endothermically and exothermically-driven properties in a single

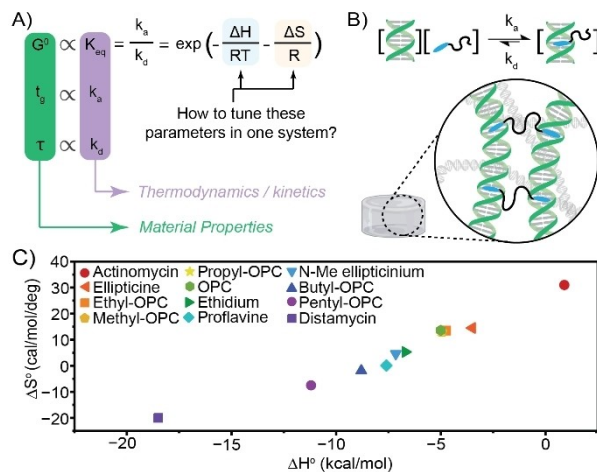


Figure 1. a) Relationship of material properties to thermodynamics properties and their corresponding enthalpy and entropy-driven interactions. The exact mathematical relations are not shown b) Schematic of a DISH displaying reversible intercalation as an inter-strand cross-linker c) Enthalpies and entropies of binding for various intercalators determined by viscometry.^[20]

[*] S. M. Hughes,[†] A. Aykanat,[†] N. G. Pierini, W. A. Paiva, A. A. Weeks, A. S. Edwards, O. C. Durant, N. J. Oldenhuis
Department of Chemistry, College of Engineering and Physical Science
University of New Hampshire
23 Academic Way, Parsons Hall, Durham, NH 03824, United States of America
E-mail: Nathan.Oldenhuis@unh.edu

[†] Denotes equal contribution

material system is an unmet challenge, which could transform the use of PSHs across a broad temperature range.

In this communication, we leverage the use of bifunctional polymeric cross-linked DNA dyes to form DNA intercalating supramolecular hydrogels (DISHs), which can be tuned to exhibit exothermic or endothermic binding in a single material system (Figure 1b).^[20,25–30] These materials display a unique and controllable thermal response through strategic selection of DNA dye, and remain functional in diverse biological and aqueous environments due to their precedence as pharmacological compounds.^[28,31]

DNA intercalators are planar aromatic compounds frequently utilized in molecular biology and anti-cancer treatments. Binding to DNA can be driven by both enthalpic forces (π - π stacking, hydrogen bonding, electrostatic interactions) and entropic forces (hydrophobicity, release of structured water), which display distinct thermodynamic binding profiles depending on the chosen intercalator.^[20,25–30] The values of ΔS° and ΔH° are dictated via a delicate interplay between the amount of structured water released and the relative strength of the enthalpic interactions of DNA/intercalator versus DNA/water (Figure 1c). We hypothesized that we could form a material, displaying both endothermically and exothermically-driven properties, by linking DNA chains with dimeric intercalators.

Small dimeric intercalators favor intra-strand binding, while intercalators bound to the ends of a long polymer should increase inter-strand binding in a sufficiently concentrated solution of dsDNA.^[32] The programmability of these DISHs should arise through careful selection of the thermodynamic or kinetic parameters of the intercalators, similar to other functional DNA hydrogels.^[33–36] However, appending the intercalators to a polymer could significantly alter their binding properties, as shown in the ellipticine series in Figure 1c. Furthermore, while translating the strength of individual exothermic bonding to bulk material properties is well-established due to the straightforward determination of ΔH° , translating endothermic bonding into structure-properties is less clear.^[8,9,37] This is because negative entropic forces, such as the formation of cross-links, can counteract entropy gain, making the direct estimation of ΔS° challenging and its relation to mechanical properties difficult.^[10,38–41]

To explore DISH materials, we developed bi-functional cross-linkers terminated with two identical dsDNA intercalators and investigated their properties when mixed with DNA. We chose derivatives of four commonly used intercalators—acridine, psoralen, thiazole orange, and phenanthridine—each differing in hydrophobicity, charge, and the size of their polycyclic aromatic groups. These derivatives can be readily accessed in sufficient quantities and appended to polymers, enabling a preliminary analysis of how structural and chemical differences among the intercalators influence their binding efficiency and mode of interaction. To maximize inter-strand interactions and maintain high water solubility, each intercalator was appended to the ends of polyethylene glycol ($M_w=2,000$, PEG_{2k}) to form four cross-linkers: Acr-PEG, Pso-PEG, Thi-PEG, and Phen-PEG (Figure 2a). Importantly, the large

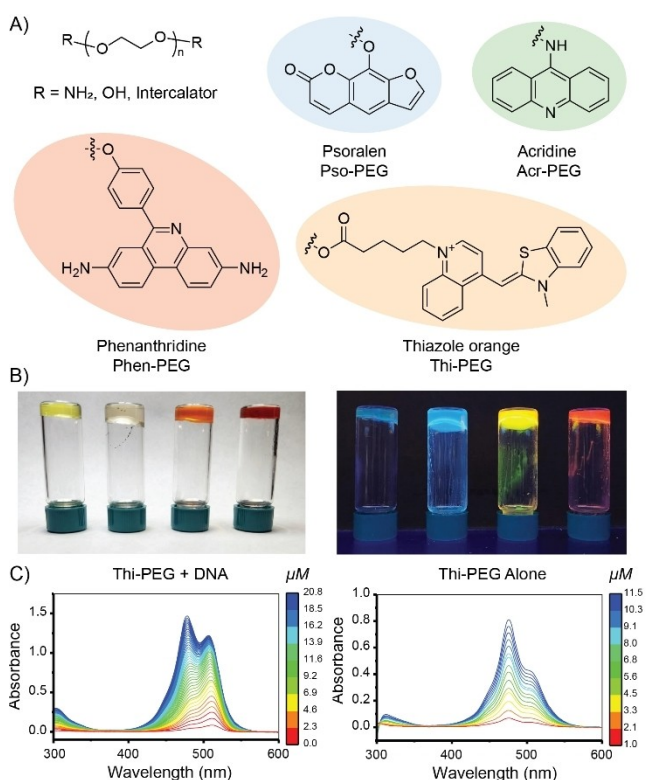


Figure 2. a) Structures of intercalators and their assigned acronyms b) Photograph of DISHs used in this study (left to right) Acr-PEG, Pso-PEG, Thi-PEG, and Phen-PEG under ambient light (left image) and 365 nm light (right image) c) UV/Vis spectra of Thi-PEG with DNA (left) and Thi-PEG in buffer (right) at increasing concentrations.

molecular weight of the bis-intercalators prevents simple transmembrane travel, rendering them relatively non-toxic.^[42]

To create a DISH, we required a readily available and inexpensive source of dsDNA. Sheared genomic DNA from biological sources (e.g., salmon milt, calf thymus) is $\sim \$100$ per gram, $> 70\%$ double-stranded, and has found use in bioplastics, membranes, and gels.^[43,44] Biomass-derived DNA materials offer broad appeal due to their biocompatibility, low environmental impact, and unique emergent properties despite the lack of sequence control.^[45] As biomass DNA materials are typically covalently cross-linked, utilizing supramolecular cross-linked DISHs would significantly expand their potential applications.^[29,31]

The DISHs were prepared by mixing solutions of genomic salmon milt DNA and cross-linker to a final concentration of 50 mg mL^{-1} (5 % w/w) and 2 mM respectively. Upon mixing, we observed an immediate change in material properties (e.g. viscosity and fluorescence) for each bi-functional cross-linker versus controls (Figure 2b). To confirm that intercalation was the operative mode of binding, UV/Vis measurements were conducted by adding $5 \mu\text{L}$ of a $40 \mu\text{M}$ solution of each cross-linker to $200 \mu\text{L}$ of a $25 \mu\text{g mL}^{-1}$ (0.0025 % w/w) DNA solution (Figure 2b–c). We observed a significant increase in fluorescence intensity or a shift in the absorbance spectra in the presence of DNA

compared to a control, suggesting intercalation was occurring (Figure S1–8).^[46] As intercalation can happen between $n - 1$ base pairs, 20 mM of bifunctional cross-linker would saturate the binding sites in the 5% w/w DNA solution (~40 mM bp). Previous studies have shown that after every other base-pair is occupied, binding affinity is markedly decreased due to insertion next to a neighboring intercalator.^[47] To avoid complex binding conditions and maintain homogeneity, we used a final cross-linker concentration of 2 mM. Empirically, higher concentrations produced stiffer DISHs, but lead to inhomogeneous incorporation into DNA (Figure S9).

Next, we investigated the mechanical properties of each DISH using shear rheology. Amplitude sweeps conducted at varying temperatures (27, 37, and 47°C) confirmed the gels were within the linear viscoelastic region (Figure S10). Due to the relatively inhomogeneous nature of salmon milt DNA, the melting temperature (T_m) is lowered to ~60°C, limiting the range of temperatures available for probing the initial DISH materials.^[48,49] Thermal behaviors across a larger temperature range have been examined; however, for the sake of consistency, this paper will primarily focus on 27°C, 37°C, and 47°C (Figure S11, S12). Shear frequency sweeps conducted at 1% strain and 37°C showed an enhancement in storage modulus (G') for Acr-PEG, Thi-PEG, and Phen-PEG versus a DNA control (Figure S13). Controls using 2 mM PEG_{2k} and PEG_{2k}-amine did not dramatically increase G' , demonstrating intercalation was necessary to form a robust material (Figure S14, S15). It should be noted that due to DNA's extreme length and relative thinness, it forms robust entanglements at very low concentrations, resulting in physical gelation.^[50] To determine if the concentration of DNA was dominating the mechanical properties, we repeated the frequency sweeps at a lower DNA concentration (2.5% w/w DNA, 2 mM Thi-PEG) and observed the same trends (Figure S16). Pso-PEG only increased G' slightly compared to the controls, suggesting acridine, thiazole orange, and phenanthridine have significantly higher K_{eq} .^[50]

To examine the thermal behavior of each DISH, frequency sweeps were conducted at 27, 37, and 47°C in triplicate. DISHs using Pso-PEG and Phen-PEG exhibited increasing viscosity with temperature, ultimately crossing over into the terminal flow regime at low angular frequencies and elevated temperatures (Figure 3a). Interestingly, Thi-PEG and Acr-PEG DISHs showed no cross-over and no shift towards the terminal flow regime at any frequency or temperature. When re-plotted as a function of $\tan \delta$, Thi-PEG and Phen-PEG DISHs show a clear increase in elasticity at high frequencies, and the Acr-PEG DISH shows an enhancement in elasticity across all frequencies, as a function of increasing temperature (Figure 3b). This correlates well with the observations of Yu et al. in their entropically cross-linked system.^[21] Finally, Pso-PEG exhibited only slight differences at high angular frequencies compared to a DNA control. Thus the K_{eq} and k_d of Pso-PEG must be too low or fast respectively to significantly impact the innate mechanical properties of the DNA solution.^[21]

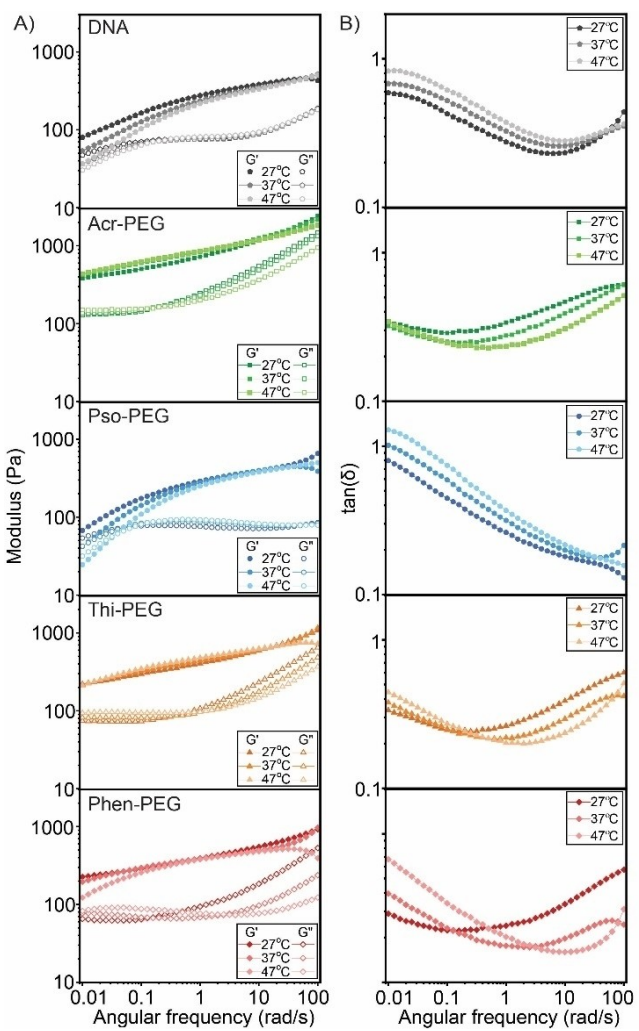


Figure 3. **a)** Representative frequency sweeps conducted at 1% strain from 0.01 to 100 rad/s at 27°C, 37°C, and 47°C. DISHs were compared to 5% (w/w) DNA sample. Top to bottom: DNA, Acr-PEG, Pso-PEG, Thi-PEG, and Phen-PEG. **b)** Frequency sweeps replotted as a function of $\tan \delta$. We note that at high frequency the effects of instrument inertia cause slight fluctuations in the observed moduli.

To corroborate these observations, stress relaxation experiments were performed on each DISH at 27, 37, and 47°C to further probe the temperature dependence of network relaxation (Figure S17). All experiments were conducted in triplicate using a freshly prepared DISH. Each stress-relaxation plot was normalized to G^0 and fit using the Kohlrausch-Williams-Watts function (KWW), $G(t)/G^0 = \exp(-t/\tau)^\beta$ (equation 1) to determine τ , where β is a fitting parameter that describes the breadth of relaxation modes (Figure 4a, S18, S19, Table S1–4). This function was selected to account for the many modes of relaxation arising from the highly polydisperse nature of salmon milt DNA, polymer entanglements, variations of local sequences, and other dynamic interactions, e.g., hydrogen bonding.^[51] Pso-PEG and Phen-PEG DISHs displayed decreasing τ with increasing temperature, while Thi-PEG showed less dependence, and Acr-PEG was invariant, or even increasing,

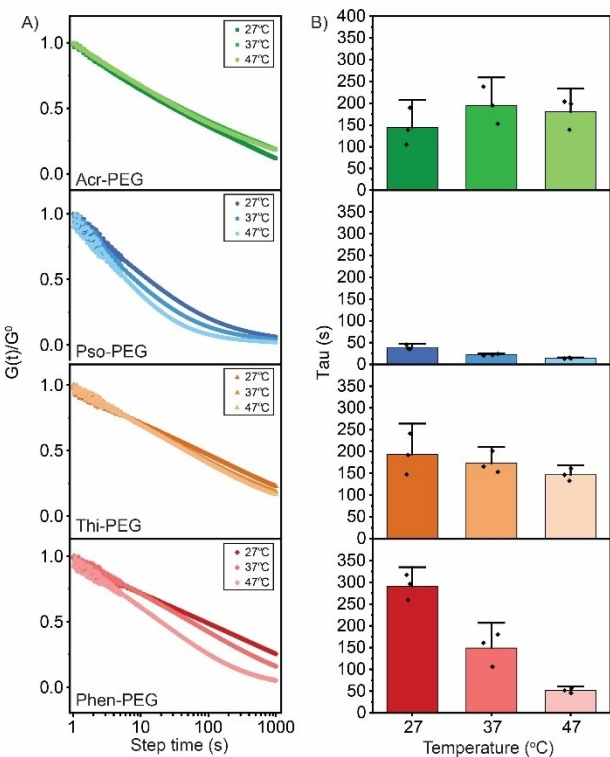


Figure 4. a) Representative normalized stress relaxation plots conducted at 2% strain and 5 rad/s. Each plot was fit to the KWW function at 27°C, 37°C, and 47°C. DISHs Top to bottom: Acr-PEG, Pso-PEG, Thi-PEG, and Phen-PEG. b) Bar graphs comparing τ values extracted from triplicate runs at temperatures 27°C, 37°C, and 47°C. Error bars represent standard error.

compared to DNA and PEG_{2k} controls (Figure 4b). These results confirm the significant influence of intercalators on the thermal stress-relaxation behaviors of the different DISHs and correlated well with what was observed in the frequency sweeps.

Interestingly, at 27°C the trend among the τ of the DISHs is Phen > Thi > Acr, at 37°C they are roughly equivalent, and at 47°C their relationship has inverted to Acr > Thi > Phen. The k_d of a physical bond has been shown to be roughly proportional to τ^{-1} of a physically linked network.^[37] Therefore, if a network is enthalpically dominated, τ should decrease with temperature, and if it is entropically dominated, τ will be invariant or inversely proportional to temperature.^[21,37] This demonstrates that τ can be tuned to decrease, remain invariant, or even increase as a function of temperature via intercalator selection. To demonstrate the tolerance of DISHs to complex mixtures of biomolecules, the above experiments were repeated with an Acr-PEG DISH containing 10% heat-treated fetal bovine serum, and no significant change in modulus or relaxation time was observed over 48 hours (Figure S20).

With agreement between the frequency sweeps and stress relaxation experiments, we next rationalized why each intercalator exhibited a unique thermal behavior. As illustrated in the ellipticine series in Figure 1, changing steric bulk can significantly alter the thermodynamics of binding.

We anticipate that the increased bulk of Pso-PEG diminished binding to DNA, and thus is challenging to observe compared to the inherent viscoelastic properties of a DNA gel. Based on the thermal responses of Thi-PEG and Phen-PEG, it seems likely that $\Delta H^\circ < 0$ and $\Delta S^\circ > 0$ for the interactions with DNA. As intercalation can be both enthalpically and entropically favored, it is reasonable to observe that τ decreases with increasing temperature due to the exothermic nature of the interaction, despite the positive entropy. We hypothesize that Thi-PEG has less enthalpic contributions and more entropic favorability due to its decreased variance with temperature. For Acr-PEG, we posit that $\Delta H^\circ > 0$ and $\Delta S^\circ > 0$, to explain the increase of τ as a function of temperature, as binding would be endothermic. Eyring analysis of this data agrees with these postulations (Figure S21, Table S5).

While there are some examples of entropically dominated intercalators, acridine and other flavin-based molecules exhibit complex binding modes, where both intercalation and minor-groove binding can occur.^[52,53] Thus, we reason that either Acr-PEG is a pure entropic intercalator or favors minor groove binding at high temperatures, which also can be entropically driven.^[54] The potential of several modes of interaction leads to a more complex thermal response, offering a wider range of control over material properties. To probe this further, we repeated the frequency sweep and stress relaxation experiments of Acr-PEG at pH 5.15, where the nitrogen of acridine is partially protonated (Figure S22). This induced a more dramatic increase of τ with temperature, suggesting that electrostatic charge can facilitate the displacement of more structured water, but cannot recoup the enthalpic energy loss from DNA-water hydrogen bonding and ion-dipole interactions.^[54] Additionally, it should be noted that the entropic contribution for specific dyes can vary depending on factors like local sequence or competing interactions with the major or minor groove. Further investigation will be pursued to establish how chemical features of each intercalator, pH, and DNA source will result in the desired mechanical and thermal response.

In this study, we have introduced DISHs capable of tunable viscoelasticity and thermal response based on DNA intercalator selection. To our knowledge, this is the first PSH system that can be tuned between exothermic and endothermic binding without dramatically altering material composition. As there are thousands of known intercalating molecules with a broad range of thermodynamic properties, it becomes possible to create a broad spectrum of materials by strategically selecting the terminal intercalating molecule. The DISHs are additionally constructed from inexpensive and abundantly studied materials. We envision that these materials could find future use as non-destructive cross-linkers to join DNA structures, forming functional biomaterials, or energy damping materials in the case of the endothermically linked Acr-PEG.

Supporting Information

The authors have cited additional references within the Supporting Information.^[55–60]

Acknowledgements

This work was supported by CIBBR (NIH, P20GM113131), NH Biomade (NSF, #IIA 1757371), NSF CAREER (DMR Biomaterials, 2340569), and NIH MIRA (1R35GM154998).

Conflict of Interest

The authors declare no conflict of interest.

Data Availability Statement

The data that support the findings of this study are available from the corresponding author upon reasonable request.

Keywords: Biomaterials · Entropy driven gelation · DNA Intercalations · Supramolecular hydrogels

[1] E. A. Appel, J. del Barrio, X. J. Loh, O. A. Scherman, *Chem. Soc. Rev.* **2012**, *41*, 6195–6214.

[2] J. Zhang, Y. Hu, Y. Li, *Gel Chemistry: Interactions, Structures and Properties*, Springer, Singapore **2018**, pp. 9–59.

[3] K. C. Bentz, S. M. Cohen, *Angew. Chem. Int. Ed.* **2018**, *57*, 14992–15001.

[4] M. J. Webber, M. W. Tibbitt, *Nat. Rev. Mater.* **2022**, *2022*, 1–16.

[5] J. L. Mann, A. C. Yu, G. Agmon, E. A. Appel, *Biomater. Sci.* **2018**, *6*, 10–37.

[6] J. L. Drury, D. J. Mooney, *Biomaterials* **2003**, *24*, 4337–4351.

[7] S. Correa, A. K. Grosskopf, H. Lopez Hernandez, D. Chan, A. C. Yu, L. M. Stapleton, E. A. Appel, *Chem. Rev.* **2021**, *121*, 11385–11457.

[8] W. C. Yount, D. M. Loveless, S. L. Craig, *J. Am. Chem. Soc.* **2005**, *127*, 14488–14496 DOI 10.1021/ja054298a.

[9] J. Chung, A. M. Kushner, A. C. Weisman, Z. Guan, *Nat. Mater.* **2014**, *13*, 1055–1062.

[10] E. A. Appel, F. Biedermann, D. Hoogland, J. Del Barrio, M. D. Driscoll, S. Hay, D. J. Wales, O. A. Scherman, *J. Am. Chem. Soc.* **2017**, *139*, 12985–12993.

[11] B. Marco-Dufort, R. Iten, M. W. Tibbitt, *J. Am. Chem. Soc.* **2020**, *142*, 15371–15385.

[12] C. H. Reynolds, M. K. Holloway, *ACS Med. Chem. Lett.* **2011**, *2*, 433–437.

[13] T. Weilandt, N. L. Löw, G. Schnakenburg, J. Daniels, M. Nieger, C. A. Schalley, A. Lützen, *Chem. Eur. J.* **2012**, *18*, 16665–16676.

[14] E. A. Appel, F. Biedermann, U. Rauwald, S. T. Jones, J. M. Zayed, O. A. Scherman, *J. Am. Chem. Soc.* **2010**, *132*, 14251–14260.

[15] C. S. Y. Tan, G. Agmon, J. Liu, D. Hoogland, E.-R. Janeček, E. A. Appel, O. A. Scherman, *Polym. Chem.* **2017**, *8*, 5336–5343.

[16] Y. Fang, S. Al-Assaf, G. O. Phillips, K. Nishinari, T. Funami, P. A. Williams, L. Li, *J. Phys. Chem. B* **2007**, *111*, 2456–2462.

[17] M. V. Rekharsky, Y. Inoue, *Chem. Rev.* **1998**, *98*, 1875–1918.

[18] P. Fischer, H. Rehage, *Langmuir* **1997**, *13*, 7012–7020.

[19] M. S. Turner, M. E. Cates, *Langmuir* **1991**, *7*, 1590–1594.

[20] M.-A. Schwaller, G. Dodin, J. Aubard, *Biopolymers* **1991**, *31*, 519–527.

[21] A. C. Yu, H. Lian, X. Kong, H. Lopez Hernandez, J. Qin, E. A. Appel, *Nat. Commun.* **2021**, *12*, 746.

[22] Y. N. Pandey, G. J. Papakonstantopoulos, M. Doxastakis, *Macromolecules* **2013**, *46*, 5097–5106.

[23] S. Kapsabelis, C. A. Prestidge, *J. Colloid Interface Sci.* **2000**, *228*, 297–305.

[24] F. Sciortino, Y. Zhang, O. Gang, S. K. Kumar, *ACS Nano* **2020**, *14*, 5628–5635.

[25] W. Zhang, B. Wu, S. Sun, P. Wu, *Nat. Commun.* **2021**, *12*, 4082.

[26] J. Wu, B. Wu, J. Xiong, S. Sun, P. Wu, *Angew. Chem.* **2022**, *134*, e202204960.

[27] S. Samanta, S. Kim, T. Saito, A. P. Sokolov, *J. Phys. Chem. B* **2021**, *125*, 9389–9401.

[28] I. Haq, *Archives of Biochemistry and Biophysics* **2002**, *403*, 1–15.

[29] H. P. Hopkins, K. A. Stevenson, W. D. Wilson, *J. Solution Chem.* **1986**, *15*, 563–579.

[30] M. Hossain, P. Giri, G. S. Kumar, *DNA Cell Biol.* **2008**, *27*, 81–90.

[31] J. B. Chaires, *Curr. Opin. Struct. Biol.* **1998**, *8*, 314–320.

[32] M. Maaloum, P. Muller, S. Harlepp, *Soft Matter* **2013**, *9*, 11233–11240.

[33] Y. Shao, H. Jia, T. Cao, D. Liu, *Acc. Chem. Res.* **2017**, *50*, 659–668.

[34] Z. Xing, C. Ness, D. Frenkel, E. Eiser, *Macromolecules* **2019**, *52*, 504–512.

[35] D. Cao, Y. Xie, J. Song, *Macromol. Rapid Commun.* **2022**, *43*, 2200281.

[36] Y. Li, R. Chen, B. Zhou, Y. Dong, D. Liu, *Adv. Mater.* **2024**, *36*, 2307129.

[37] D. M. Loveless, S. L. Jeon, S. L. Craig, *Macromolecules* **2005**, *38*, 10171–10177.

[38] M. Rubinstein, R. H. Colby, *Polymer Physics*, Oxford University Press **2003**.

[39] T. C. Lubensky, *Solid State Commun.* **1997**, *102*, 187–197.

[40] A. A. Gusev, F. Schwarz, *Macromolecules* **2019**, *52*, 9445–9455.

[41] O. K. Vorov, D. R. Livesay, D. J. Jacobs, *Entropy* **2008**, *10*, 285–308.

[42] N. J. Yang, M. J. Hinner, *Methods Mol. Biol.* **2015**, *1266*, 29–53.

[43] J. Han, Y. Guo, H. Wang, K. Zhang, D. Yang, *J. Am. Chem. Soc.* **2021**, *143*, 19486–19497.

[44] D. Wang, J. Cui, M. Gan, Z. Xue, J. Wang, P. Liu, Y. Hu, Y. Pardo, S. Hamada, D. Yang, D. Luo, *J. Am. Chem. Soc.* **2020**, *142*, 10114–10124.

[45] D. Wang, P. Liu, D. Luo, *Angew. Chem.* **2022**, *134*, e202110666.

[46] A. L. Benvin, Y. Creeger, G. W. Fisher, B. Ballou, A. S. Waggoner, B. A. Armitage, *J. Am. Chem. Soc.* **2007**, *129*, 2025–2034.

[47] J. Dikic, R. Seidel, *Biophys. J.* **2019**, *116*, 1394–1405.

[48] K. A. Heinrichs, *Adv. Biochem. Biotechnol.* **2017**.

[49] F. Ma, Y. Ma, C. Du, X. Yang, R. Shen, *Journal of Molecular Structure* **2015**, *1100*, 154–161.

[50] K. Regan, S. Ricketts, R. M. Robertson-Anderson, *Polymer* **2016**, *8*, 336.

[51] A. Lukichev, *Phys. Lett. A* **2019**, *383*, 2983–2987.

[52] J. B. Chaires, *Arch. Biochem. Biophys.* **2006**, *453*, 26–31.

[53] H.-K. Kim, J.-M. Kim, S. K. Kim, A. Rodger, B. Nordén, *Biochemistry* **1996**, *35*, 1187–1194.

[54] H. Y. Alniss, *J. Med. Chem.* **2019**, *62*, 385–402.

[55] G. R. Fulmer, A. J. M. Miller, N. H. Sherden, H. E. Gottlieb, A. Nudelman, B. M. Stoltz, J. E. Bercaw, K. I. Goldberg, *Organometallics* **2010**, *29*, 2176–2179.

[56] J. Yan, P. F. Marina, A. Blencowe, *Polymer* **2021**, *13*, 1403.

[57] C. Zhou, V. X. Truong, Y. Qu, T. Lithgow, G. Fu, J. S. Forsythe, *J. Polym. Sci. Part A* **2016**, *54*, 656–667.

[58] A. D. Buhimschi, D. M. Gooden, H. Jing, D. R. Fels, K. S. Hansen, W. F. Beyer Jr, M. W. Dewhirst, H. Walder, F. P. Gasparro, *Photochem. Photobiol.* **2020**, *96*, 1014–1031.

[59] J. R. Carreon, K. M. Stewart, K. P. Mahon, S. Shin, S. O. Kelley, *Bioorg. Med. Chem. Lett.* **2007**, *17*, 5182–5185.

[60] H. Egami, S. Nakagawa, Y. Katsura, M. Kanazawa, S. Nishiyama, T. Sakai, Y. Arano, H. Tsukada, O. Inoue, K. Todoroki, Y. Hamashima, *Org. Biomol. Chem.* **2020**, *18*, 2387–2391.

Manuscript received: June 12, 2024

Accepted manuscript online: August 5, 2024

Version of record online: September 29, 2024